

Neutron Structure Analysis and Structural Disorder of Poly(*p*-phenylene benzobisoxazole)

Yasuhiro Takahashi

Department of Macromolecular Science, Graduate School of Science, Osaka University, Toyonaka, Osaka, 560, Japan

Received August 13, 1998; Revised Manuscript Received April 9, 1999

ABSTRACT: On the X-ray fiber diagram of poly(*p*-phenylene benzobisoxazole) (PBO), the diffuse streak scatterings are observed along the first and third layer lines, while Laue spots can be observed on the second and fourth layer lines. This shows that the molecular heights of PBO are disordered by a half of the fiber period. Therefore, the cell parameter *c* reduces to a half of the fiber period, 12.05 Å. Furthermore, all the reflections observed on the X-ray fiber diagram can be indexed by the one-chain unit cell with parameters *a* = 5.651 Å, *b* = 3.570 Å, and $\gamma = 101.4^\circ$ (at 295 K). Neutron diffraction measurements were made on the equator at 17, 100, 200, and 295 K, and the structure analyses were made. The half-widths of the reflections do not depend on the temperature. This shows that the crystallite size and lattice distortion are independent of the temperature. The temperature dependences of the unit cell dimensions and temperature parameter are small in comparison with those of polyethylene, one of the flexible polymers. This may reflect the rigidity of the PBO molecule.

Introduction

Poly(*p*-phenylene benzobisoxazole) (PBO) is known as a strong polymer and a polymer of the highest modulus.¹ Its properties are mainly attributed to the molecular rigidity of PBO (Figure 1). X-ray crystal analysis of PBO was carried out by Fratini et al.² They reported that two molecular chains pass through a monoclinic unit cell with parameters *a* = 11.20 Å, *b* = 3.540 Å, *c* = 12.05 Å, and $\gamma = 101.3^\circ$ and that PBO includes a considerable amount of axial disorder. Thereafter, Martin and Thomas³ reported the disordered structure of PBO, where they attributed the diffuse scattering to Laue spots,⁴ and recently, Tashiro et al.⁵ reported the computer simulation of the fiber pattern of PBO, where they also attributed the diffuse scattering to the superlattice spots.⁴

Neutron diffraction has several advantages^{6–8} in comparison with X-ray diffraction. Accordingly, new information about crystal structure could be obtained differing from the X-ray work. The scattering length of an atom is independent of the atomic number. Accordingly, hydrogen and deuterium have different scattering lengths for neutron diffraction, although for X-ray diffraction, they have the same scattering length. Furthermore, the scattering lengths by neutron diffraction are independent of the scattering angle θ . The intensities of the reflections with large θ values can be observed strongly and can be measured accurately. This is especially an advantage for crystalline polymers, in which the reflection intensities become rapidly weak with the angle θ because of the disorder in the crystalline region and the low degree of orientation. Absorption of neutrons by most elements, for example, aluminum, is very small. Therefore, the apparatus for low- and high-temperature measurements can be easily designed, and the measurements at low and high temperature are easy.

The purpose of the present study is to clarify the structure of PBO in the crystalline region, including the disorder. As the results of the present study, all the observed reflections can be indexed by one-chain unit

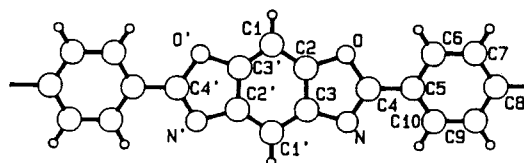


Figure 1. Chemical structure of poly(*p*-phenylene benzobisoxazole) and numbering of atoms.

cell with parameters *a* = 5.651 Å, *b* = 3.570 Å, *c* = 6.03 Å, and $\gamma = 101.4^\circ$ (at 295 K). The heights of PBO molecules are disordered by a half of fiber period, 12.05 Å. The temperature dependences of the unit cell parameters and structure are not so large as those of polyethylene, which may be attributed to the rigidity of PBO molecule.

Experimental Section

X-ray measurements were made by Cu K α radiation monochromatized by a pyrolyzed graphite. Fiber diagrams were taken by using the cylindrical camera with 4.5 cm radius and the vacuum camera with 10.0 cm radius. The specimen for X-ray diffraction measurements was made by arranging the fibers (Toyobo Co. Ltd.) in a cylindrical bundle about 0.5 mm in diameter.

Neutron diffraction measurements were carried out by a powder diffractometer (HERMES) equipped with JRR-3M installed by the Japan Atomic Energy Research Institute (JAERI) using $\lambda = 1.8196$ Å. The specimen was made by arranging the fibers in a cylindrical bundle about 10 mm in diameter, covered by vanadium foil, and set into the aluminum sample tube with 6.5 cm diameter. Intensity distributions in the range $5^\circ \leq 2\theta \leq 150^\circ$ on the equator were measured at 17, 100, 200, and 295 K. Numbers of the observed reflections at 17, 100, 200, and 295 K are 11, 11, 12, and 12, respectively. In Figure 2, the intensity distribution measured at 17 K is shown. Integrated intensities were estimated by measuring the areas of the reflections, where the overlapped reflections of 010 and $\bar{1}10$ were separated under the assumption of the Lorentz profile.

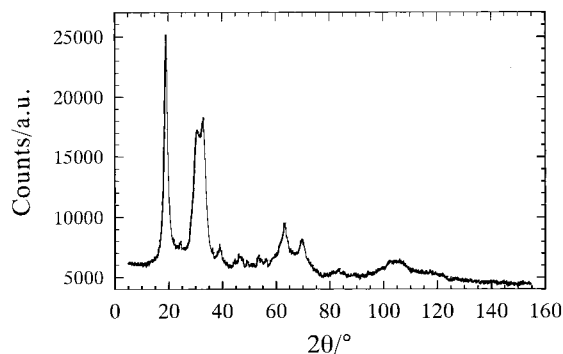


Figure 2. Neutron intensity distribution on the equator of poly(*p*-phenylene benzobisoxazole) measured at 17 K.

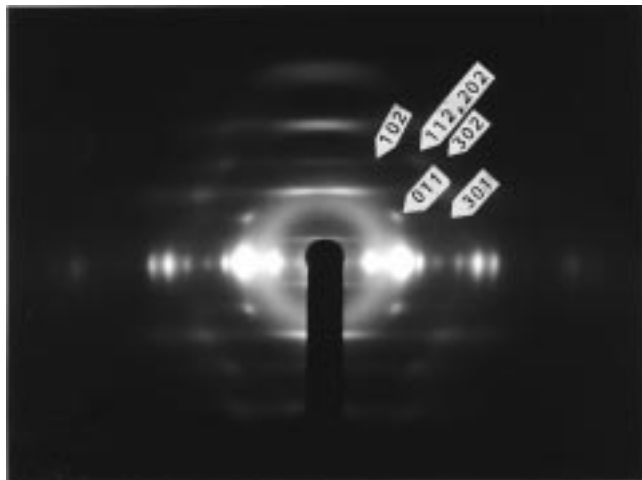


Figure 3. X-ray fiber diagram of poly(*p*-phenylene benzobisoxazole).

Results and Discussion

Unit Cell and Structural Disorder. On the X-ray fiber diagrams (Figure 3), diffuse streak scatterings are observed along the first and third layer lines, and several diffraction spots can be observed on the second and fourth layer lines. All the observed diffraction spots can be satisfactorily indexed by a one-chain unit cell with parameters $a = 5.651 \text{ \AA}$, $b = 3.570 \text{ \AA}$, and $\gamma = 101.4^\circ$, the a parameter of which is half of that reported by Fratini et al.² Furthermore, the c parameter should be reduced to half, 6.03 \AA , of the fiber period 12.05 \AA , which Fratini et al.² reported for the c parameters, because diffraction spots cannot be observed on the odd numbers of the layer lines. The space group is considered to be $Pm\bar{C}_s^1$ from the symmetry of the molecule. Since the diffraction spots can be observed only on the even numbers of the layer lines, the molecular heights of PBO should be disordered by $1/2$ along the molecular axis; the phenylene is substituted by the benzobisoxazole. This can be called a kind of the substitutional disorder. Any systematic relations among the diffraction spots were not observed on the second and fourth layer lines. Accordingly, this disorder exists in both the a and b directions. The diffuse scattering intensity is given by following equation

$$I_{\text{diffuse}} = \langle |F|^2 \rangle - |\langle F \rangle|^2$$

where F is the structure factor and $\langle \rangle$ indicates an average. When the molecular structure factor is F_M ,

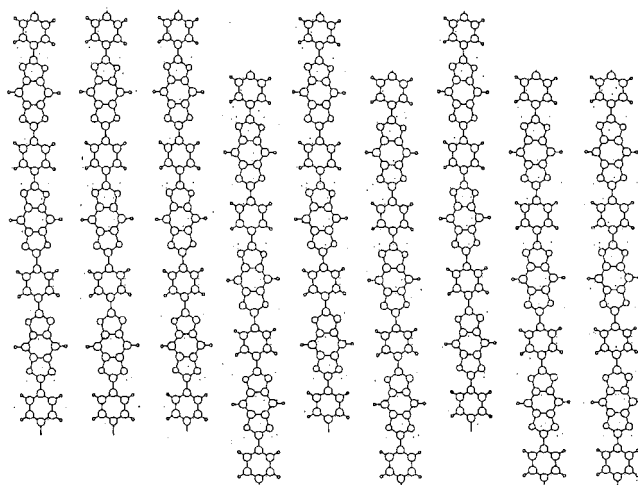


Figure 4. Schematic representation of disorder in poly(*p*-phenylene benzobisoxazole).

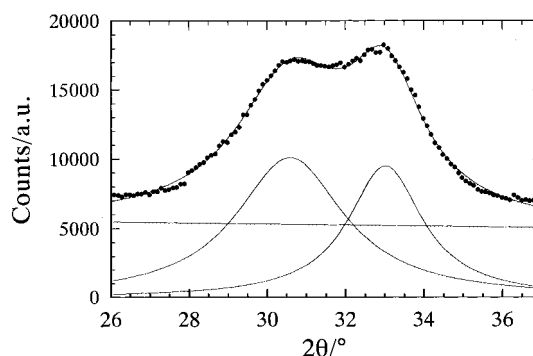


Figure 5. Curve resolution of the intensity profile of 010 and $\bar{1}10$ at 17 K by the Lorentz function.

$\langle |F|^2 \rangle$ and $\langle F \rangle$ are given as follows:

$$\langle |F|^2 \rangle = |F_M|^2$$

$$\langle F \rangle = \frac{1}{2} F_M \exp(\pi i l / 2) + \frac{1}{2} F_M \exp(-\pi i l / 2) = F_M \cos(\pi l / 2)$$

Accordingly,

$$\begin{aligned} I_{\text{diffuse}} &= |F_M|^2 \{1 - \cos(\pi l / 2)\} \{1 + \cos(\pi l / 2)\} \\ &= 0 \quad \text{when } l = 2n \\ &= |F_M|^2 \quad \text{when } l = 2n + 1 \end{aligned}$$

Intensity distributions on the odd numbers of the layer lines are given by the square of the molecular structure factor. The disorder in PBO is schematically shown in Figure 4. This type of disorder was already found in the case of the planar zigzag form of poly-oxacyclobutane,⁹ where the oxygen is substituted by the methylene.

Temperature Dependences of Unit Cell Dimensions and Half-Widths of Reflections. On the intensity distribution of the equator, two reflections 010 and $\bar{1}10$ overlap each other. The intensity profile of 100 was satisfactorily approximated by a Lorentz function. Therefore, the overlapped reflection was resolved to two reflections under the assumption of the Lorentz profile. Curve resolution of the intensity profile at 17 K is shown in Figure 5. Unit cell parameters a , b , and γ were determined by the 2θ values of three reflections 100,

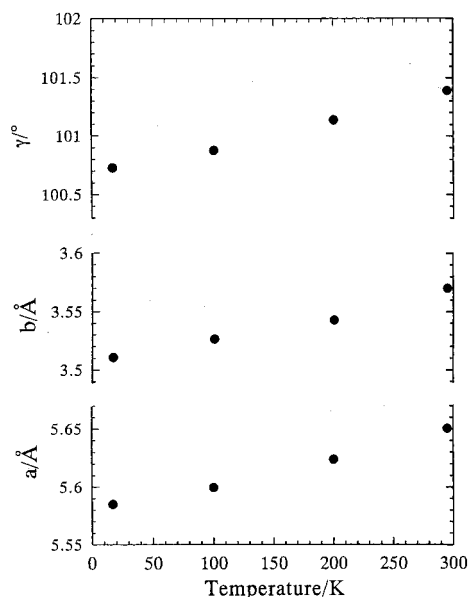


Figure 6. Temperature dependences of unit cell parameters.

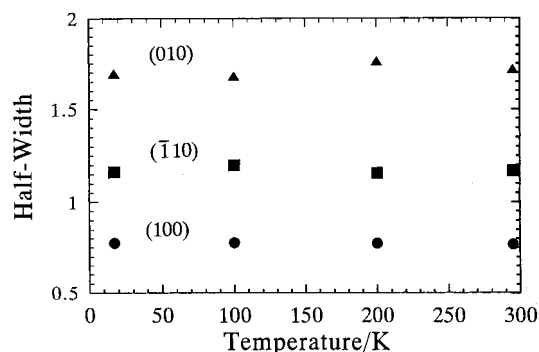


Figure 7. Temperature dependences of half-width of reflections 100, 010, and 110.

Table 1. Temperature Dependence of Unit Cell Parameters

	17 K	100 K	200 K	295 K
<i>a</i> (Å)	5.585	5.600	5.624	5.651
<i>b</i> (Å)	3.511	3.527	3.543	3.570
γ (deg)	100.73	100.88	101.14	101.39

010, and 110. The temperature dependences of the unit cell parameters are given in Table 1 and shown in Figure 6, which are not so large as those of polyethylene⁶ and poly(vinyl alcohol).⁷ This may be attributed to the rigidity of PBO molecule. The half-widths of the reflections are plotted in Figure 7, which are independent of the temperature. The reflection 100 is sharp, while 010 is broad. This suggests that the crystallite of PBO assumes a rectangular form long in the *a* direction, and the size is independent of the temperature. The half-width of the reflection is also reflected by the lattice distortion. Accordingly, the lattice distortion of PBO is also independent of the temperature.

Neutron Structure Analysis. The constrained least-squares method¹⁰ was applied to the refinement of the crystal structure of PBO. The refinements were started from the crystal structure reported by Fratini et al.² During the refinements, the bond lengths and bond angles were fixed on the generally accepted values² (Table 2). The hydrogen atom of benzobisoxazole was chosen as the origin of the molecule (Figure 1). Accordingly, the variable parameters to be refined are the scale

Table 2. Fixed Bond Lengths (Å) and Bond Angles (deg) in the Constrained Least-Squares Refinements

bond length		bond angle	
C2–O	1.383	C2–O–C4	104.1
C4–O	1.370	C3–N–C4	104.4
C3–N	1.399	C2–C1–C3'	112.5
C4–N	1.300	C1–C2–O	127.0
C1–C2	1.385	C3–C2–O	107.1
C1–C3	1.385	C1–C2–C3	125.8
C2–C3	1.405	C1'–C3–N	129.7
C4–C5	1.464	C2–C3–N	108.6
C5–C6	1.387	C1'–C3–C2	121.7
C5–C10	1.387	N–C4–O	115.6
C6–C7	1.387	C5–C4–O	122.2
C7–C8	1.387	C5–C4–N	122.2
C8–C9	1.387	C4–C5–C6	120.0
C9–C10	1.387	C4–C5–C10	120.0
		C6–C5–C10	120.0
		C5–C6–C9	120.0
		C6–C7–C8	120.0
		C7–C8–C9	120.0
		C8–C9–C10	120.0
		C9–C10–C5	120.0

^a Numbering of atoms is given in Figure 1. ^b C–H distances are fixed at 1.09 Å.

Table 3. Atomic Parameters Finally Obtained by the Constrained Least-Squares Refinements

	17 K	100 K	200 K	295 K
ϕ^a (deg)	−169.6 (2.8)	−170.9 (2.3)	−172.4 (2.8)	−172.6 (2.3)
τ^b (deg)	193.4 (8.4)	201.7 (5.8)	203.6 (7.2)	205.7 (5.8)
<i>B</i> (Å ²)	1.96 (1.99)	1.89 (1.56)	2.14 (2.03)	2.14 (1.77)
<i>R</i> factor (%)	9.85	9.47	13.14	12.08

^a The azimuthal angle of benzobisoxazole with respect to the line perpendicular to the *b* axis. ^b The internal rotation angle N–C4–C5–C10. The standard deviations are given in parentheses.

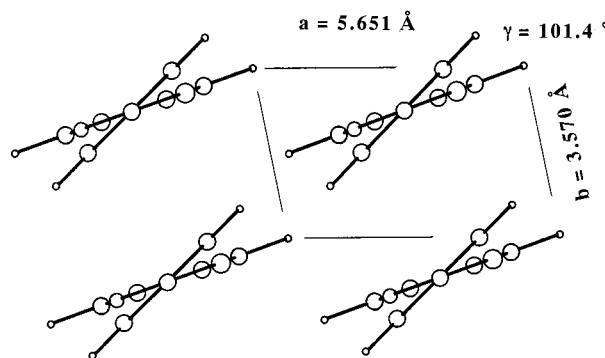


Figure 8. Crystal structure of poly(*p*-phenylene benzobisoxazole) at 295 K.

factor, the azimuthal angle of benzobisoxazole with respect to the line perpendicular to the *b* axis, ϕ , the internal rotation angle N–C4–C5–C10, τ , and the overall temperature parameter, *B* (Table 2). The *R* factor converged to 9.9%, 9.5%, 13.1%, and 12.1% for the intensity data at 17, 100, 200, and 295 K, respectively. The parameters and standard deviations finally obtained by the constrained least-squares refinements are given in Table 3. The fractional coordinates of the atoms are given in Table 4. The comparison between the observed and calculated structure factors is given in Table 5. The crystal structure of PBO at 295 K is shown in Figure 8. The temperature dependences of the azimuthal angle ϕ , the internal rotation angle τ , and the overall isotropic temperature parameter *B* are plotted in Figures 9, 10, and 11, respectively. The azimuthal angle ϕ and the internal rotation angle τ

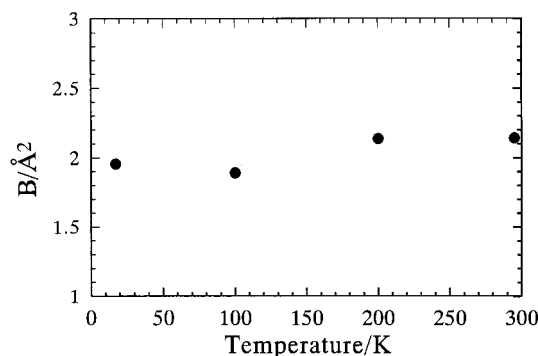


Figure 9. Temperature dependence of isotropic temperature parameter.

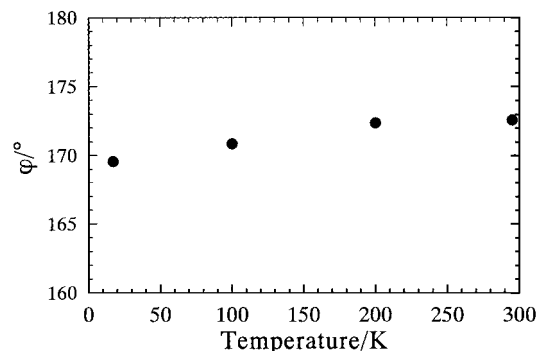


Figure 10. Temperature dependence of the azimuthal angle of the molecule ϕ .

Table 4. Atomic Parameters in Fractional Coordinates

	<i>x</i>	<i>y</i>	<i>z</i>		<i>x</i>	<i>y</i>	<i>z</i>
(a) 17 K							
H1	0.000	0.000	0.000	N	-0.672	-0.392	0.203
C1	-0.195	-0.114	0.000	C4	-0.477	-0.278	0.262
C2	-0.341	-0.198	0.093	C5	-0.481	-0.280	0.384
O	-0.267	-0.156	0.203	C6	-0.683	-0.478	0.440
C3	-0.592	-0.345	0.093	H6	-0.839	-0.633	0.393
C1'	-0.738	-0.430	0.000	C10	-0.282	-0.084	0.442
H1'	-0.933	-0.544	0.000	H10	-0.123	0.072	0.398
(b) 100 K							
H1	0.000	0.000	0.000	N	-0.674	-0.369	0.203
C1	-0.196	-0.107	0.000	C4	-0.478	-0.261	0.261
C2	-0.341	-0.186	0.093	C5	-0.482	-0.263	0.383
O	-0.267	-0.146	0.202	C6	-0.671	-0.495	0.439
C3	-0.594	-0.325	0.093	H6	-0.817	-0.676	0.393
C1'	-0.740	-0.404	0.000	C10	-0.295	-0.033	0.442
H1'	-0.936	-0.512	0.000	H10	-0.146	0.149	0.398
(c) 200 K							
H1	0.000	0.000	0.000	N	-0.677	-0.342	0.203
C1	-0.197	-0.099	0.000	C4	-0.480	-0.242	0.261
C2	-0.342	-0.173	0.093	C5	-0.483	-0.244	0.383
O	-0.268	-0.136	0.202	C6	-0.672	-0.478	0.439
C3	-0.596	-0.301	0.093	H6	-0.818	-0.660	0.393
C1'	-0.742	-0.375	0.000	C10	-0.298	-0.012	0.442
H1'	-0.939	-0.474	0.000	H10	-0.150	0.172	0.398
(d) 295 K							
H1	0.000	0.000	0.000	N	-0.677	-0.337	0.203
C1	-0.197	-0.098	0.000	C4	-0.480	-0.239	0.261
C2	-0.342	-0.171	0.093	C5	-0.484	-0.241	0.383
O	-0.269	-0.134	0.202	C6	-0.669	-0.483	0.439
C3	-0.596	-0.297	0.093	H6	-0.811	-0.672	0.393
C1'	-0.743	-0.370	0.000	C10	-0.302	-0.001	0.442
H1'	-0.940	-0.468	0.000	H10	-0.157	0.189	0.397

decrease as the temperature decreases. The temperature parameter B slightly decreases as the temperature decreases. This might be reflected by the rigidity of the PBO molecule and is consistent with the slight change of the unit cell parameters (Figure 6). The quantum

Table 5. Comparison between the Observed and Calculated Structure Factors

index	$\sqrt{I_o}$	$\sqrt{I_c}$	index	$\sqrt{I_o}$	$\sqrt{I_c}$
(a) 17 K					
100	114.02	108.12	320	57.54	57.83
010	153.68	134.10	410		
110	127.63	130.94	400		
110	45.28	50.73	220		
200			410	149.92	143.54
210	49.09	56.71	420		
210	41.80	70.77	130		
300	140.54	151.78	030		
310			320	79.00	84.54
120			230		
020			510		
220	131.53	124.11	500		
120			130	21.36	13.54
310			330		
			520		
(b) 100 K					
100	113.86	108.19	320	52.72	54.36
010	150.51	133.40	410		
110	129.32	131.07	400		
110	39.08	44.08	220		
200			410	120.35	116.24
210	46.22	51.89	420		
210	39.90	70.19	130		
300	127.90	138.61	030		
310			320	75.92	80.54
120			230		
020			510		
220	119.07	114.83	500		
120			130	21.05	13.71
310			330		
			520		
(c) 200 K					
100	115.97	107.61	320	56.81	49.93
010	159.84	134.04	410		
110	124.18	128.98	400		
110	41.10	42.65	220		
200			410	116.82	109.01
210	46.40	45.89	420		
210	34.72	70.05	130		
300	119.49	135.85	030		
310			320	59.25	71.59
120			230		
020			510		
220	101.43	98.64	500		
120			130	20.74	13.20
310			330		
			520		
(d) 295 K					
100	114.97	107.58	320	52.87	46.55
010	155.48	133.26	410		
110	125.14	129.35	400		
110	39.38	40.50	220		
200			410	109.10	104.59
210	48.94	44.23	420		
210	37.34	70.02	130		
300	117.90	130.87	030		
310			320	63.14	70.79
120			230		
020			510		
220	95.75	96.71	500		
120			130	24.52	13.43
310			330		
			520		

mechanical calculation of low molecular weight model compounds of PBO suggests that the PBO molecule assumes the planar structure.^{11–13} Actually, the PBO molecule deviates from the planar structure from $\tau = 13^\circ$ to 26° dependent on the temperature. The difference between the actual and theoretical structures may be attributed to the assumptions that the theoretical calculations are based on.

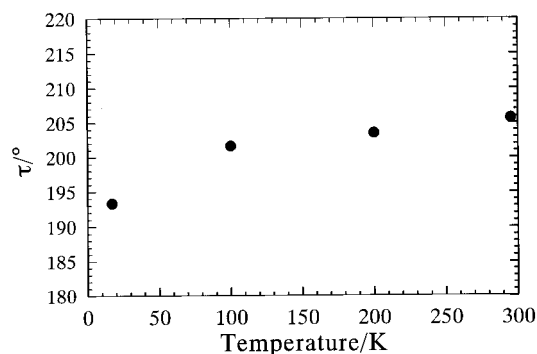


Figure 11. Temperature dependence of the internal rotation angle τ .

In comparison with the sum of van der Waals radii, three intermolecular short contacts can be found in the disordered PBO structure (295 K). Two short distances 1.95 and 1.83 Å are found between hydrogen atoms of phenylene rings and between those of benzobisoxazole rings of two molecules arranged in the [110] direction, respectively. The short distance 2.20 Å is found between hydrogen and carbon atoms of benzobisoxazole rings of two molecules arranged in the [100] direction. These short intermolecular contacts may bring about the deviation from the exactly registered disordered structure, i.e., the diffuse streak scatterings on the even numbers of layer lines with higher orders.

On the c projection, the structure of PBO is essentially the same as that proposed by Fratini et al.² Fratini et al. reported that the angle between the benzobisoxazole and phenyl rings is 13°. But the present neutron structure analysis shows $25.7 \pm 5.8^\circ$ (295 K). Neutron diffraction has several advantages⁶⁻⁸ in comparison with X-ray diffraction. The scattering lengths by neutron diffraction are independent of the scattering angle

θ . The intensities of the reflections with large θ values can be observed strongly and can be measured accurately. Furthermore, the scattering length of the hydrogen atom by neutron diffraction (−3.739, 5.803, 6.646, and 9.360 for H, C, O, and N atoms, respectively) is larger than by X-ray diffraction (1, 6, 8, and 7 for H, C, O, and N atoms, respectively). Generally, the hydrogen atoms are located on the outer shell of the molecule. Accordingly, the neutron structure analysis of polymer gives the more accurate azimuthal angle of the molecule and the atomic group, i.e., a more accurate structure than X-ray structure analysis.

Acknowledgment. I thank Prof. M. Ohashi of Tohoku University (at present, Yamagata University) for neutron diffraction measurements.

References and Notes

- (1) Krause, S. J.; Haddock, T. B.; Vezie, D. L.; Lenhert, P. G.; Hwang, W. F.; Price, G. E.; Helminiak, T. E.; O'Brien, J. F.; Adams, W. W. *Polymer* **1988**, *29*, 1354.
- (2) Fratini, A. V.; Lenhert, P. G.; Resch, T. J.; Adams, W. W. *Mater. Res. Soc. Symp. Proc.* **1989**, *134*, 431.
- (3) Martin, D. C.; Thomas, E. L. *Macromolecules* **1991**, *24*, 2450.
- (4) Guinier, A. X-ray Diffraction. In *Crystals, Imperfect Crystals, and Amorphous Bodies*; Dover Publications: New York, 1994.
- (5) Tashiro, K.; Yoshino, J.; Kitayama, T.; Yabuki, K. *Macromolecules* **1998**, *31*, 5430.
- (6) Bacon, G. E. *Neutron Diffraction*; Clarendon Press: Oxford, 1975.
- (7) Takahashi, Y. *J. Polym. Sci., Part B: Polym. Phys.* **1997**, *35*, 193.
- (8) Takahashi, Y. *Macromolecules* **1998**, *31*, 3868.
- (9) Takahashi, Y.; Osaki, Y.; Tadokoro, H. *J. Polym. Sci., Polym. Phys. Ed.* **1981**, *19*, 1153.
- (10) Takahashi, Y.; Sato, T.; Tadokoro, H.; Tanaka, Y. *J. Polym. Sci., Polym. Phys. Ed.* **1973**, *11*, 233.
- (11) Welsh, W. J.; Mark, J. E. *J. Mater. Sci.* **1983**, *18*, 1119.
- (12) Welsh, W. J.; Yang, Y. *Comput. Polym. Sci.* **1991**, *1*, 139.
- (13) Yang, Y.; Welsh, W. J. *Macromolecules* **1990**, *23*, 2410.

MA981282E